

## $\beta$ -decay of $^{22}\text{O}$

L Weissman<sup>1,5</sup>, A F Lisetskiy<sup>1</sup>, O Arndt<sup>2</sup>, U Bergmann<sup>3,6</sup>, B A Brown<sup>1</sup>,  
J Cederkall<sup>3,7</sup>, I Dillmann<sup>2</sup>, O Hallmann<sup>2</sup>, L Fraile<sup>3</sup>, S Franchoo<sup>3,4</sup>,  
L Gaudefroy<sup>4</sup>, U Köster<sup>3</sup>, K-L Kratz<sup>2</sup>, B Pfeiffer<sup>2</sup>, O Sorlin<sup>4</sup> and  
ISOLDE collaboration

<sup>1</sup> NSCL, Michigan State University, East Lansing, MI 48824, USA

<sup>2</sup> Institut für Kernchemie, Universität Mainz, Mainz-55128, Germany

<sup>3</sup> ISOLDE, CERN, CH-1211 Geneva 23, Switzerland

<sup>4</sup> Institut de Physique Nucléaire d'Orsay, F-91406 Orsay Cedex, France

E-mail: Leonid.weissman@uconn.edu

Received 18 January 2005

Published 21 April 2005

Online at [stacks.iop.org/JPhysG/31/553](http://stacks.iop.org/JPhysG/31/553)

### Abstract

A mass-separated  $^{12}\text{C}^{22}\text{O}$  molecular ion beam from the ISOLDE facility was used to study the decay of neutron-rich  $^{22}\text{O}$ . The experimental results were compared with the results from an earlier experiment and predictions by shell-model calculations using various effective interactions. The mechanism leading to the vanishing decay strength to the first  $1^+$  level of the  $^{22}\text{F}$  nucleus, predicted with the USD effective interaction but not supported by the experimental data, is analysed.

### 1. Introduction

Shell-model calculations for nuclei in the sd-shell were developed two decades ago and have proven to be quite reliable. One can have considerable confidence in the theoretical predictions for the sd-shell nuclei that are not far from the stability. The Gamow–Teller transitions of sd-shell nuclei with five or more excess neutrons have been calculated in [1] utilizing the USD interaction [2]. The growing amount of experimental information on nuclei from the sd-shell, which has become available since the publication of [1], shows that the calculations reproduce well the energies of the excitation levels of the daughter nuclei, the decay half-lives and the decay feeding patterns. However, there are a few cases where the experimental results are in strong contradiction with the theory. One of these is the  $\beta$ -decay of the  $^{22}\text{O}$  nucleus. The allowed decay from the  $0^+$  ground state proceeds to  $1^+$  excited levels in the  $^{22}\text{F}$  daughter nucleus. The calculations predict a very weak allowed decay to the first  $1^+$  excited level with

<sup>5</sup> Author to whom any correspondence should be addressed.

<sup>6</sup> Present address: Paul Scherrer Institut, 5232 Villigen PSI, Switzerland.

<sup>7</sup> Present address: Physics Department, Lund University, Lund, Sweden.

a branching ratio of 0.04% (Table IV in [1]). Such a weak branching ratio ( $\log ft$  value of 7.5) is unusual for allowed decays and may indicate a potentially interesting physics case. The only experimental study of the decay of  $^{22}\text{O}$  was performed at the LISE fragment separator at GANIL laboratory [3–5]. The experiment showed a good agreement with the calculated  $^{22}\text{F}$  excitation spectrum and the calculated half-life. However, an intense (up to 34%) feeding to the first  $1_1^+$  level was observed. The strong contradiction between the experiment and the theory was emphasized in [5, 6] but no satisfactory explanation was proposed.

Measurements with fragmentation beams may suffer from strong background since an admixture of several fragmentation products is sent to a detector setup. In this regard, a measurement at an ISOL facility can have advantages provided that a pure  $^{22}\text{O}$  beam is obtained. In this correspondence we report on a measurement performed at the ISOLDE facility with the purpose of verifying the results of the earlier experiment and understanding the strong contradiction with the prediction of the USD calculations.

## 2. Experiment and results

Neutron-rich  $^{22}\text{O}$  nuclei were produced in very asymmetric fission reactions induced by 1.4 GeV protons ( $3 \times 10^{13}$  protons per pulse) bombarding a standard ISOLDE uranium carbide graphite target heated to 2000 °C. The target was connected to a MK-7 plasma ion source to ionize the radioactive atoms diffused from the target. A water cooled line between the target and the ion source served for condensation of all radioactive products except gaseous elements and compounds. Oxygen was extracted as a CO molecular ionic beam [7]. A  $^{12}\text{C}^{22}\text{O}$  ion beam was extracted and mass-separated. The leakage of non-gaseous isobars through the cooled line was negligible. A weak  $^{13}\text{C}^{21}\text{O}$  beam that could not be mass-separated from  $^{12}\text{C}^{22}\text{O}$  was the only contaminant at mass  $M = 34$ . The isotopic abundance of  $^{13}\text{C}$  is only 1.1%; however, the production of the  $^{21}\text{O}$  isotope in the target is a few times higher than the corresponding production of  $^{22}\text{O}$ . Thus the total intensity of the contamination was of the order of 5%. The  $^{22}\text{O}$  yield was estimated to be 3000 ions per proton pulse [7].

A detailed description of the detector setup and its calibrations can be found in our previous publication [8]. The extracted and mass-separated  $^{12}\text{C}^{22}\text{O}$  ions were implanted into an aluminized tape. The implantation point was surrounded by Kapton windows and thin plastic scintillators with a total detection efficiency for beta particles of 35(4)%. Two germanium detectors of 75% and 65% relative efficiency were placed in close geometry around the implantation point. The efficiencies of the detectors were calibrated using sources produced and collected on-line.

The  $\beta$ -gated  $\gamma$ -spectrum collected at mass  $M = 34$  for approximately 700 proton pulses on the target is shown in figure 1. The 1.1 s beam-on implantation time followed 4.8 s beam-off decay period. The purity of the obtained  $^{22}\text{O}$  source allows one to identify practically all transitions in the spectrum. The 72, 638, 710, 918 and 1862 keV  $^{22}\text{O}$  transitions reported in [5] are readily observed. The energies of some of the transitions observed in the spectrum, 710, 990, 1934 and 2499 keV, suggest that they are, at least in part, due to the summing of the strong  $\gamma$ -ray lines, 72 and 638 keV, 72 and 918 keV, 72 and 1862 keV, 1862 and 638 keV, respectively. The  $\gamma$ - $\gamma$  coincidence spectra obtained by applying gates on the known strongest  $^{22}\text{O}$  transitions show that the weak 944, 2499 keV transitions belong to the  $^{22}\text{O}$  decay cascade (figure 2). The time decay curves gated by the strongest  $\gamma$ -transitions of interest are shown in figure 3 and the results of the fitting are presented in table 1. The time behaviour of the 944, 990, 1934 and 2499 keV weak  $\gamma$ -lines is consistent with the half-lives shown in table 1. The relative intensities of the  $^{22}\text{O}$  transitions that are not pure summing lines (see the text below) are shown in table 1 together with their observed coincidence relations.

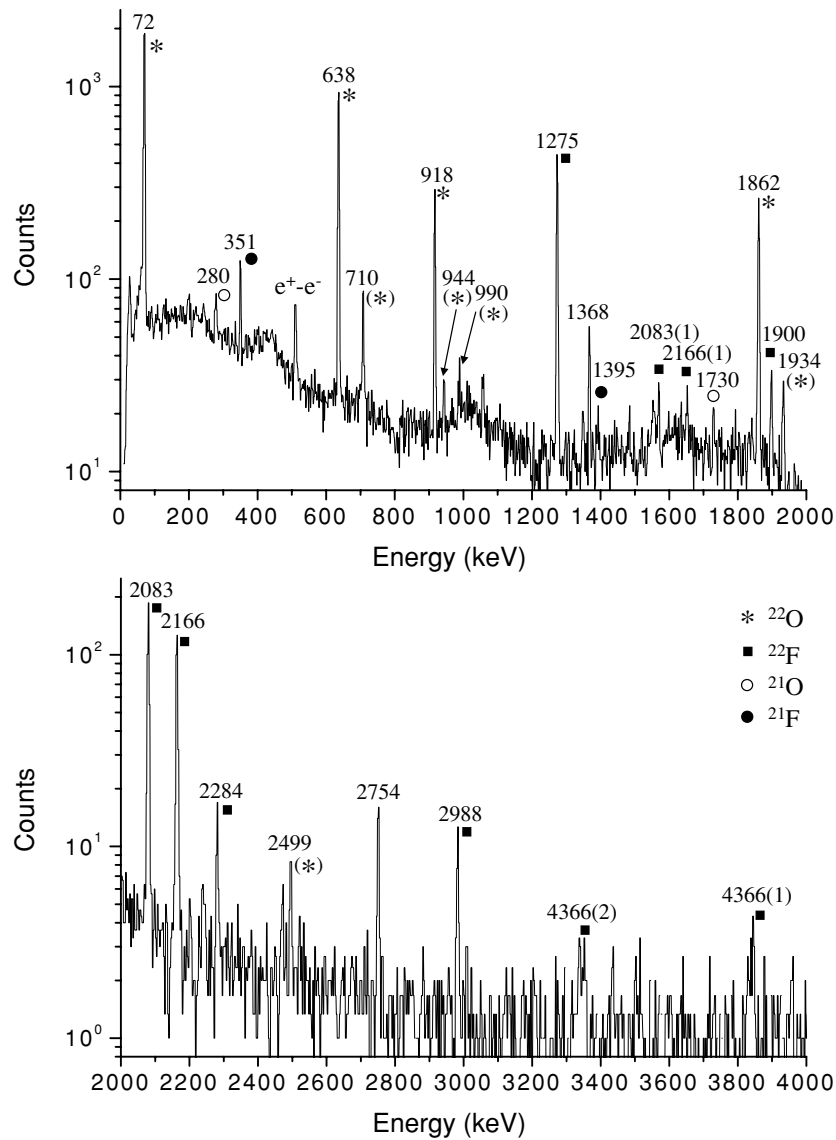


**Figure 1.**  $\beta$ -gated  $\gamma$ -spectrum collected for the  $M = 34$  separator mass value is shown. The  $\gamma$ -rays belonging to the  $^{22,21}\text{O}$  and  $^{22,21}\text{F}$  decays are indicated by asterisks, open circles, full squares and full circles respectively. The escape peaks of the strong 2083, 2166 and 4366 keV transitions are also shown. The asterisk symbols in parentheses are newly observed  $^{22}\text{O}$  transitions or possibly summed transitions.

Except for the  $\gamma$ -lines from the  $^{22}\text{O}$  decay, the transitions belonging to the decay of the  $^{22}\text{F}$  daughter nucleus are observed in the spectrum. Weak 351, 1395 keV and 280, 1730 keV  $\gamma$ -rays from the  $^{21}\text{O}$  and  $^{21}\text{F}$  decays respectively are also seen in the spectrum. Two escape peaks of the strong  $^{22}\text{F}$ , 4366 keV,  $\gamma$ -ray are seen. The weak 1368 and 2754 keV  $\gamma$ -ray transitions observed in the spectrum are due to a longer-lived  $^{24}\text{Na}$  contamination that is the decay product of a  $^{24}\text{Ne}$  beam used for calibration of the setup. We have not observed the 1874 keV transition reported in [5] nor the 260 keV level reported in [9].

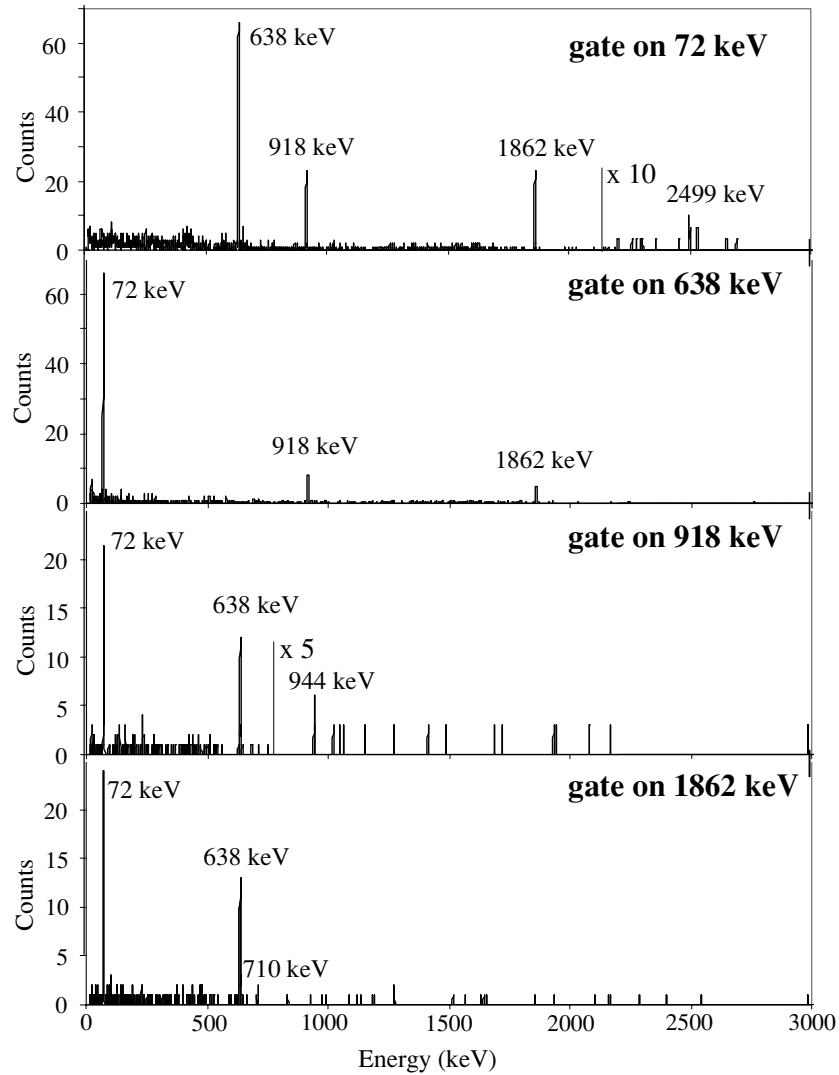


**Figure 2.** Background-subtracted coincidence spectra obtained by applying gates on the 72, 638, 918 and 1862 keV transitions.

### 3. Discussion

The decay scheme of the  $^{22}\text{O}$  is presented in figure 4(a). The ordering of the levels is in accordance with the results of earlier decay [5] and reaction [6, 9, 10] studies. The strong cascade of the 1862, 918, 638 and 72 keV  $\gamma$  transitions results in summing effects in the germanium detectors placed in close geometry around the source. GEANT simulations [11] based on the decay scheme (figure 3(a)) show that the effective detection efficiency for these transitions is reduced by 15–20%. The simulations also show that within the experimental errors the summing of 72 and 638 keV transitions accounts for the full intensity of the 710 keV line in the  $\gamma$ -spectra. According to the simulations approximately half of the intensity of the 2499 keV  $\gamma$ -line is due to the summing of the 638 and 1862 keV transitions. The relative

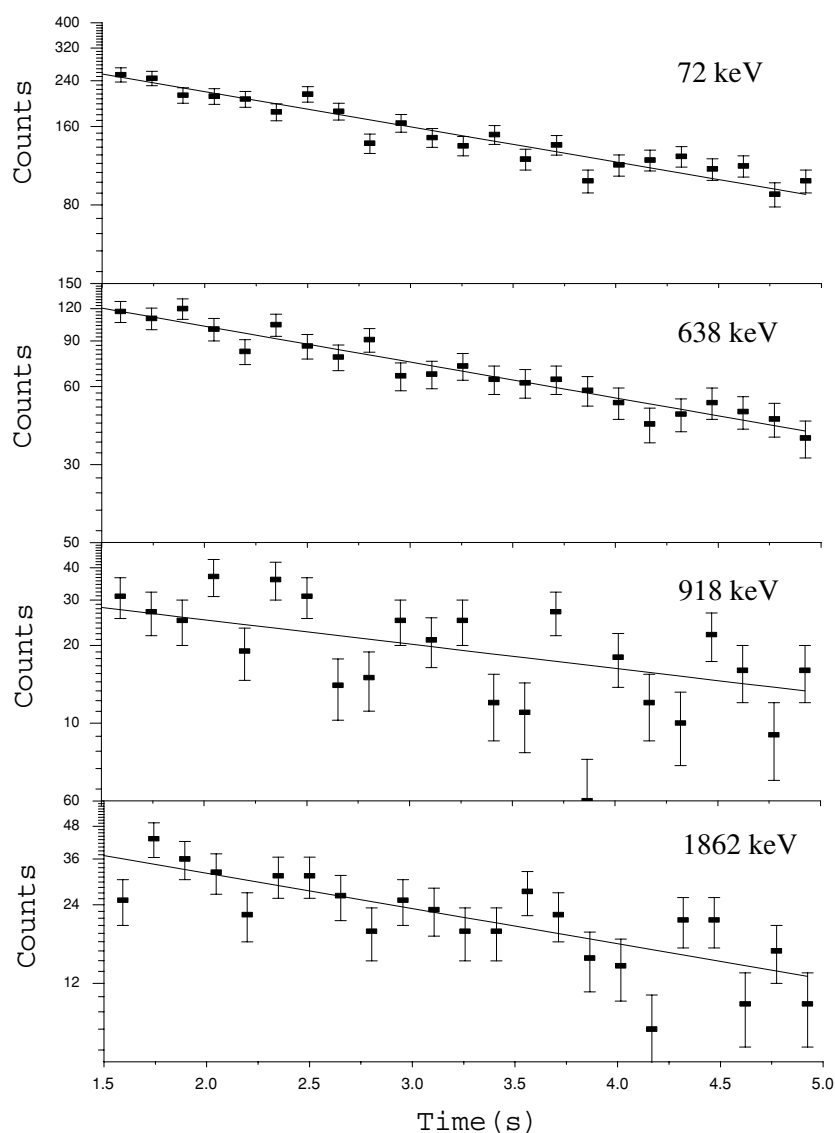


**Figure 3.** The results of fitting the decay curves gated by the  $\gamma$ -ray transitions of interest.

intensities of the  $^{22}\text{O}$  transitions presented in table 1 are corrected for detector efficiencies and for the summing effects. The intensities of the 1275, 2085 and 2166 keV  $\gamma$ -transitions from the  $^{22}\text{F}$  decay represent 100%, 85% and 68% of the total  $^{22}\text{O}$  decay flux respectively. The averaged intensity of these transitions corrected by the corresponding branching ratios is 95(6) in the units of table 1, that is, within the errors, the same as the intensities of the 72 and 638 keV transitions. This indicates that all the  $^{22}\text{O}$  decay flux proceeds via levels lying above the 710 keV state. The adopted half-life, 2.25(9) s, is in agreement with [5] and in contradiction with the earlier measurement [12]. The presence of the  $^{21}\text{O}^{13}\text{C}$  contaminant in the beam made it impossible to determine the neutron emission probability of  $^{22}\text{O}$ . The intensity of the

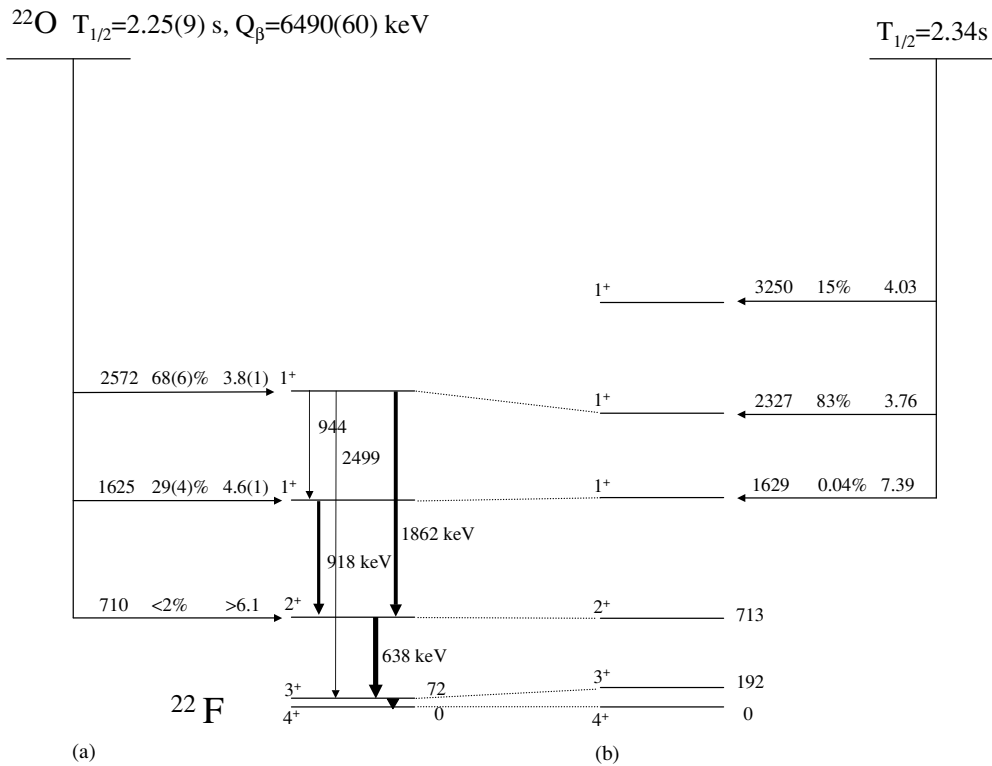


**Figure 4.** (a) The  $^{22}\text{O}$  decay scheme deduced from this work. The  $Q_{\beta}$  value is taken from [13]. (b) The result of shell-model calculations utilizing USD interactions [2].

**Table 1.** The relative intensities, observed coincidences and deduced half-life for the  $^{22}\text{O}$   $\gamma$ -transitions. The relative intensity of the 1274.5 keV, 2082.5 keV and 2166 keV transitions from the  $^{22}\text{F}$  decay is also shown.

$E$ (keV)	Relative intensity	Observed coincidences	Half-life (ms)
72	100	638, 918, 1862, 2499	2280(120)
638	98(10)	72, 918, 1862	2180(150)
918	33(5)	72, 638, 944	2940(600)
944	3(1)		
1862	63(7)	72, 638, 710	2160(300)
2499	1.5(10)		
1274.5	99(10)		
2082.5	78(8)		
2166	63(8)		

351 keV  $^{21}\text{F}$  transition was consistent with an assumption that most of the  $^{21}\text{F}$  nuclei originated from the contaminant beam rather than from neutron emission in the  $^{22}\text{O}$  decay.

In general, the results of the present measurement support the findings of the earlier experiment [5]. More detailed information on the  $^{22}\text{O}$  decay, obtained in this work, enforces the confrontation between the experiment and the results of the USD shell-model calculations from [1] (see figures 4(a) and (b)).

**Table 2.** The comparison of the experimental level energies, decay branching ratios (BR) and  $B(\text{GT}; 0^+ \rightarrow 1_n^+)$  values with the results of the shell-model calculations utilizing different interactions. Quenching factor of 0.77 for GT matrix elements is used in calculations.

	$T_{1/2}$ (s)	$1_1^+$			$1_2^+$			$1_3^+$		
		$E$ (keV)	BR (%)	B(GT)	$E$ (keV)	BR (%)	B(GT)	$E$ (keV)	BR (%)	B(GT)
Experiment	2.25(9)	1625	29(4)	0.10(1)	2572	68(6)	0.61(8)	Not observed		
USD (W)	2.34	1629	0.04	0.0001	2327	83	0.54	3250	15	0.30
CW	2.45	1476	45	0.12	2429	53	0.37	3139	0.2	0.003
HBUSD	2.54	1290	13	0.03	2417	79	0.53	2710	3	0.03
HBUMSD	2.06	1589	37	0.13	2455	56	0.48	3185	2	0.04
USD(3)	3.15	2431	23	0.12	2902	74	0.70	4259	3	0.22

**Table 3.** Comparison of the one-body contributions  $j_i \rightarrow j_f$  to the total matrix element (GT m.e.) of Gamow–Teller decay to the  $1_1^+$  state in  $^{22}\text{F}$  calculated with USD(W), CW, HBUSD and HBUMSD interactions. USD(1) and USD(2) correspond to the USD interaction with the effective single-particle  $\epsilon(d_{3/2})$  energy (eff. spe) raised by 1 MeV and 2 MeV, respectively. USD(3) corresponds to the USD interaction with the single-particle  $\epsilon(d_{3/2})$  and  $\epsilon(s_{1/2})$  energies raised by 1.3 MeV and 0.7 MeV respectively.

Interaction	eff. spe			$d_{5/2} \rightarrow d_{5/2}$	$d_{3/2} \rightarrow d_{5/2}$	$s_{1/2} \rightarrow s_{1/2}$	$d_{3/2} \rightarrow d_{3/2}$	GT m.e.	B(GT)
	$\epsilon(d_{3/2})$	$\epsilon(s_{1/2})$	$\epsilon(d_{3/2})$						
USD (W)	-6.79	-2.45	0.03	-0.61	0.22	0.40	0.002	0.015	0.0001
CW	-6.49	-2.61	0.49	-1.02	0.18	0.38	0.007	-0.452	0.12
HBUSD	-6.86	-3.10	0.54	-0.86	0.16	0.48	0.00	-0.22	0.028
HBUMSD	-6.98	-2.69	0.76	-1.23	0.43	0.32	0.01	-0.47	0.13
USD(1)	-6.79	-2.45	1.03	-0.64	0.17	0.41	0.002	-0.05	0.001
USD(2)	-6.79	-2.45	2.03	-0.66	0.12	0.40	0.001	-0.14	0.011
USD(3)	-6.79	-1.75	1.33	-1.20	0.49	0.25	0.004	-0.46	0.13

In fact, several effective interactions have been developed for the sd-shell region. Some of these effective interactions, USD (or W) [1], CW [14], HBUSD and HBUMSD (SDPOTA and SDPOTB in the original publication [15]), are implemented in the latest version of the OXBASH code [16]. In order to investigate closely the problem we have performed calculations of the  $^{22}\text{O}$  decay using all four interactions available in the code. The calculated energies and decay branches for the three lowest  $1^+$  levels are presented in table 2. Surprisingly only the calculation using the USD interaction predicts a very weak feeding of the  $1_1^+$  level. For the other three calculations the branching ratio of the decay to this level ranges from 13% to 47%, which is in qualitative agreement with the experiment.

The shell-model calculations with the different interactions yield the similar excitation energies of the three lowest  $1^+$  states in  $^{22}\text{F}$ . Therefore, the small branching ratio for the  $1_1^+$  state calculated with the USD interaction originates from the small calculated Gamow–Teller strength value, B(GT) (table 2). In order to understand the vanishing of the calculated GT strength, we have analysed and compared the one-body contributions to the total GT matrix element for the four interactions in table 3. One may note from table 3 that there is almost complete accidental cancellation of the relatively large  $d_{5/2} \rightarrow d_{5/2}$  (-0.61) contribution and cumulative  $d_{5/2} \rightarrow d_{3/2}$  and  $s_{1/2} \rightarrow s_{1/2}$  (0.62) contributions in the case of the USD interaction for the  $1_1^+$  state. The other interactions yield similar cumulative contributions of  $d_{5/2} \rightarrow d_{3/2}$  and  $s_{1/2} \rightarrow s_{1/2}$  channels but somewhat larger contribution of the  $d_{5/2} \rightarrow d_{5/2}$  channel, resulting

in a much larger total GT matrix element, and hence, better agreement with the experiment. Thus, the decay strength to the  $1_1^+$  state is balanced by several interplaying contributions, where the direct  $d_{5/2} \rightarrow d_{5/2}$  contribution is required to be larger than the contributions of the remaining parts. The balance of the contributions is sensitive to the energies of the single-particle orbitals. To test the sensitivity of the USD model to the energy of the orbitals, we have performed calculations with the USD interaction with an artificially increased energy of the  $d_{3/2}$  orbital by 1 MeV, and then by 2 MeV (USD(1) and USD(2) correspondingly in table 3). We notice a moderate increase of the  $d_{5/2} \rightarrow d_{5/2}$  channel contribution and decrease of the  $d_{5/2} \rightarrow d_{3/2}$  contribution. The total GT matrix element has increased by two orders of magnitude with the increase of the  $d_{3/2}$  orbital by 2 MeV. Additional improvement can be achieved by varying the single-particle energies for the  $d_{3/2}$  and  $s_{1/2}$  orbitals within the USD interaction. For example, we find that additional increase in  $B(\text{GT})$  by an order of magnitude may be achieved by using the USD interaction with the energies of the  $d_{3/2}$  and  $s_{1/2}$  orbitals raised by 1.3 MeV and 0.7 MeV respectively (see USD(3) line in table 3). One can see from table 2 that the calculated USD(3) strengths of decays to the  $1_2^+$  and  $1_3^+$  levels are also in better agreement with the experiment than the corresponding results obtained with USD. However, the modifications with orbital energies implemented in the USD(3) lead to worse agreement with experimental excitation energies and half-life (see USD(3) line in table 2).

This points to a rather complicated mechanism that causes the effect of vanishing of  $B(\text{GT})$  of the decay to  $1_1^+$  in the case of the USD model. The changes in the single-particle energies discussed above may indicate different properties of the two-body matrix elements in the USD and other interactions. The origin of this difference presents a complicated question and detailed study is necessary for its further understanding.

Interestingly, there are quite a few other cases where the allowed decays to the lowest levels in the daughter nuclei calculated with the USD interaction are strongly suppressed (for example, the calculated decays of  $^{21,27}\text{O}$  and  $^{23,28,29}\text{F}$  nuclei in Table IV of [1]). It would be interesting to examine all these cases in order to verify whether this is a common feature of the shell-model calculations utilizing the USD interaction related to the accidental cancellation discussed above.

All four models in table 2 predict a rather low-lying  $1_3^+$  level. The decay from this level to the  $2_1^+$  state or  $3_1^+$  states would lead to the emission of a 2–2.5 or 3.2–2.7 MeV  $\gamma$ -ray. The fact that we do not observe such a level suggests that either the  $1_3^+$  level exists at a much higher energy, or it is populated with a weak branching ratio less than 2%. The latter possibility is in agreement with the results of the calculations using the CW, HBUSD and HBMUSD interactions (table 2).

The 1874 keV transition with relative intensity of 8(4) in the units of table 1 was reported in [5]. The authors of [5] argued that it might be a transition from the  $1_3^+$  to the  $2^+$  state. This would suggest existence of two close  $1^+$  states with energies 2572 and 2584 keV, one of which would be the ‘intruder’ similar to that discussed for  $^{20}\text{O}$  decay [17]. The fact that the 1874 keV has not been observed in the present work does not support this argument.

#### 4. Conclusion

A pure  $^{12}\text{C}^{22}\text{O}$  beam was produced at the ISOLDE facility. The high quality of the beam allowed one to obtain more detailed experimental information on the  $^{22}\text{O}$  decay. The anomalously low calculated value for the intensity of the allowed decay to the  $1_1^+$  level seems to be a specific feature of the shell model using the effective USD interaction which underestimates the  $d_{5/2} \rightarrow d_{5/2}$  contribution in the total GT matrix element. Thus, this broadly used interaction should be used with some caution for calculations of decays strength. Further



study is needed to elucidate this problem. The results of calculations using other effective interactions integrated into the OXBASH code reproduce well the main decay features.

### Acknowledgments

We would like to thank the crew of the PSB-ISOLDE facility for operation of the separator and the ion source. We are grateful to Dr W F Mueller for his assistance in performing GEANT simulations. We would like to acknowledge financial support by the European commission contract numbers HPRI-CT-1999-00018, HPRI-CT-2001-50033 and the NSF grant number PHY-0244453.

### References

- [1] Wildenthal B H, Curtin M S and Brown B A 1983 *Phys. Rev. C* **28** 1343
- [2] Brown B A and Wildenthal B H 1988 *Annu. Rev. Nucl. Part. Sci.* **38** 29
- [3] Dufour J P *et al* 1986 *Z. Phys. A* **324** 487
- [4] Dufour J P *et al* 1988 *Proc. 3rd Int. Conf. on Nucleus–Nucleus Collisions (Saint-Malo, France, 1988)* ed C Esteve, C Gregoire, D Guerreau and B Tamain (Centre de Publications de L'Universite de Caen) p 25
- [5] Hubert F *et al* 1989 *Z. Phys. A* **333** 237
- [6] Orr N A, Fifield L K, Catford W N and Woods C L 1989 *Nucl. Phys. A* **491** 457
- [7] Koester U *et al* 2004 *Proc. Int. ENAM'04, Eur. Phys. J. A Direct*
- [8] Weissman L *et al* 2004 *Phys. Rev. C* **70** 024304
- [9] Clarke N M *et al* 1988 *J. Phys. G: Nucl. Phys.* **14** 1399
- [10] Stokes R H and Young P G 1969 *Phys. Rev.* **178** 1789
- [11] Agostinelli S *et al* 2003 *Nucl. Instrum. Methods A* **506** 250–303
- [12] Murphy M J, Symons T J M, Westfall G D and Crawford H J 1982 *Phys. Rev. Lett.* **49** 455
- [13] Audi G, Wapstra A H and Thibault C 2003 *Nucl. Phys. A* **727** 337
- [14] Chung W 1976 *PhD Thesis* Michigan State University  
Wildenthal B H and Chung W *Mesons in Nuclei* vol 2 ed M Rho and D Wilkinson (Amsterdam: North-Holland) p 722
- [15] Brown B A, Richter W A, Julies R E and Wildenthal B H 1988 *Ann. Phys.* **182** 191
- [16] <ftp://ftp.nsl.msui.edu/pub/oxbash>
- [17] Alburger D E, Wang G and Warburton E K 1987 *Phys. Rev. C* **35** 1479